

DOE/SF/78003--T9

MASTER

LIQUID-METAL FAST-BREEDER-REACTOR PROGRAM

REFERENCE FUEL STUDIES

FOURTH QUARTERLY REPORT
MARCH ——— JULY 1975

DOE/SF/78003--T9

DE82 005383

AT03-76SF78003

US ENERGY RESEARCH & DEVELOPMENT ADMINISTRATION
CONTRACT AT (04-3)-893 TASK 3

NOTICE

PORTIONS OF THIS REPORT ARE ILLEGIBLE. It
has been reproduced from the best available
copy to permit the broadest possible avail-
ability.

He dtd 8/22/75
filed 893/3/8-2

DISTRIBUTION OF THIS DOCUMENT IS UNLIMITED

DISCLAIMER

This report was prepared as an account of work sponsored by an agency of the United States Government. Neither the United States Government nor any agency Thereof, nor any of their employees, makes any warranty, express or implied, or assumes any legal liability or responsibility for the accuracy, completeness, or usefulness of any information, apparatus, product, or process disclosed, or represents that its use would not infringe privately owned rights. Reference herein to any specific commercial product, process, or service by trade name, trademark, manufacturer, or otherwise does not necessarily constitute or imply its endorsement, recommendation, or favoring by the United States Government or any agency thereof. The views and opinions of authors expressed herein do not necessarily state or reflect those of the United States Government or any agency thereof.

DISCLAIMER

Portions of this document may be illegible in electronic image products. Images are produced from the best available original document.

DOE/SF/78003-T9

REFERENCE FUEL STUDIES
FOURTH QUARTERLY REPORT
MARCH - JULY 1975

Approved: *P. R. Pluta in FRP*

P.R. Pluta, Manager
Reactor Engineering Section

Approved: *P. E. Bohaboy in PETS*

P.E. Bohaboy
Program Manager

NOTICE

**PORTIONS OF THIS REPORT ARE ILLEGIBLE. It
has been reproduced from the best available
copy to permit the broadest possible avail-
ability.**


Prepared for the
United States Atomic Energy Commission
Under Contract No. AT(04-3)-893
Task 3

DISCLAIMER

This book was prepared as an account of work sponsored by an agency of the United States Government. Neither the United States Government nor any agency thereof, nor any of their employees, makes any warranty, express or implied, or assumes any legal liability or responsibility for the accuracy, completeness, or usefulness of any information, apparatus, product, or process disclosed, or represents that its use would not infringe privately owned rights. Reference herein to any specific commercial product, process, or service by trade name, trademark, manufacturer, or otherwise, does not necessarily constitute or imply its endorsement, recommendation, or favoring by the United States Government or any agency thereof. The views and opinions of authors expressed herein do not necessarily state or reflect those of the United States Government or any agency thereof.

FAST BREEDER REACTOR DEPARTMENT • GENERAL ELECTRIC COMPANY
SUNNYVALE, CALIFORNIA 94086

DISTRIBUTION OF THIS DOCUMENT IS UNLIMITED



NOTICE

This report was prepared as an account of work sponsored by the United States Government. Neither the United States nor The United States Atomic Energy Commission, nor any of their employees, nor any of their contractors, subcontractors, or their employees, makes any warranty, express or implied, or assumes any legal liability or responsibility for the accuracy, completeness or usefulness of any information, apparatus, product or process disclosed, or represents that its use would not infringe privately owned rights.

TABLE OF CONTENTS

	<u>Page</u>
ABSTRACT	1
SUMMARY	1
1. FUEL ROD ENGINEERING	1
1.1 Fuel Rod Design Methods	1
1.1.1 LIFE Code Development	1
1.1.2 Transient Analysis	1
1.2 Fuel Rod Data Evaluation	1
1.2.1 Fuel Rod Failures	1
1.2.2 Fuel Rod Cladding Inelastic Strain	1
1.2.3 Fuel Rod Thermal Performance	1
1.3 Fuel and Structural Material Properties Design Correlations	1
1.3.1 Thermal Conductivity of (U,Pu)O _{2-x} Fuels	1
1.3.2 Oxygen Redistribution and Thermal Performance	1
REFERENCES	1
MAJOR CONTRIBUTORS	1
2. FUELS IRRADIATION TESTING AND ANALYSIS	1
2.1 High Burnup Irradiations	1
MAJOR CONTRIBUTORS	1

LIST OF ILLUSTRATIONS

<u>Figure</u>	<u>Title</u>	<u>Page</u>
1-1	LIFE-III Gap Conductance	
1-2	Radial Distribution of Circumferential Creep Strain	
1-3	Conditions During \$3/Second Design Transient	
1-4	LIFE-III Analysis of GE F20 Rods	

LIST OF TABLES

<u>Table</u>	<u>Title</u>	<u>Page</u>
1-1	Results of LIFE-III Calibration	
1-2	Fuel Creep Map with Grain Size = F(Temp).	
1-3	Ring Number Sensitivity Study	
1-4	LIFE-III Checkout Mechanical Analysis Rods	
1-5	Summary of Design Basis Transient Calculations for a Typical LMFBR	
1-6	F20 Power-to-Melt Experiment LIFE-III Analysis	

ABSTRACT

Task 3 of Contract AT(04-3)-893 consists of the following programs:

1. A thermodynamic data program involving plutonia and urania at high temperatures,
2. Fuel Rod Engineering,
3. Fuel Rod Test program.

The three parts are closely interrelated and are in combination aimed at providing a sound basis for the design and performance evaluation of LMFBR mixed oxide fuel rods. All three parts are continuations of ongoing work which has been underway for several years.

Previously reported results from these programs can be obtained in the following General Electric documents

GEAP-12533	August 1974
GEAP-10028-51,	August 1974
GEAP-14032-1.	November 1974

SUMMARY

FUEL ROD ENGINEERING - 189 NO. SG008

The calibration of LIFE-III has been reviewed and endorsed as satisfactory by the national working group. Phase I of the LIFE-III checkout is in progress. Critical studies of four models in the code which were substantially changed during the calibration work were completed. Preliminary sensitivity results indicate little sensitivity to mesh size, but noticeable sensitivity to operating conditions within the expected range of uncertainties.

Preliminary development requirements for LIFE-IV have been defined by the LIFE Working Group. The program will emphasize the development of new and improved fuel models to characterize behavior during the complete range of normal operation.

The LIFE code is being evaluated for possible extension to cover analysis of design basis transients up to cladding breach.

Analysis of a terminated $3/\text{second}$ transient overpower event in a typical LMFBR indicates that there is little or no fuel melting, no cladding melting, and no sodium boiling. This simplifies the modeling requirements of the national transient code.

A topical report on the analysis of the experimental encapsulated oxide fuel rods which failed during the Run 55-Run 56 power change in EBR-II is in publication.

The fuel-cladding mechanical interaction code GRO-II was modified to include the thermal expansion of the inviscid zone as a loading mechanism.

Analysis of the F20 experiment using LIFE-III is in progress. The F20 post-irradiation examination data recently completed under the Fuel Rod Testing Program, 189 #SG009, has been distributed to participants in the National Experiment Evaluation Program (F20-NEEP).

The report "Cladding Inelastic Strain in Mixed Oxide Fuel Rods: Literature Review and Data Compilation" was sent to RRD.

A submittal to the Nuclear Systems Materials Handbook entitled "Thermal Conductivity of $UO_2 - PuO_2$ " was completed, and internal review initiated. The thermal conductivity correlation will be used to estimate the effect of oxygen redistribution on fuel thermal performance.

189 NO. SG008 - FUEL ROD ENGINEERING

Cognizant Engineer: B. L. Harbourne

The purpose of this program is to establish the design basis and margins for sound, reliable fuel rods as specified in the LMFBR Program Plan, Task 6-211-3. This program will support the upgraded design, safety and economics of FTR, CRBRP and Commercial fuel rods. Steady and non-steady state fuel rod design analysis methods will be developed, evaluated and used to predict the performance of the fuel rod designs typical of these plants as well as EBR-II. Fuel rod test data will be analyzed and evaluated. The results of the data analyses will be used to provide the technical justification for design analysis methods, design criteria and operating limits for fuel rods for both steady and non-steady state conditions. Design correlations and models for fuel and structural material properties will be developed and technically justified.

1.1 FUEL ROD DESIGN METHODS

1.1.1 LIFE Code Development

The calibration of LIFE-III was completed by WARD and ANL with GE support. The end-of-life comparisons of cladding inelastic strains, center void sizes and fission gas release (Table 1-1) showed satisfactory agreement between code predictions and experimental observations on the six fuel rods. The cladding inelastic strain results are characterized by good agreement for the three CW 316 rods (WSA-2/13, WSA-2/17 and P23A-25) and underprediction for the two high burnup ST-316 rods (F9A-5 and F2V).

In addition to the obvious end-of-life data comparisons, critical studies were made of the four models in the code which were substantially changed during the calibration work. These are:

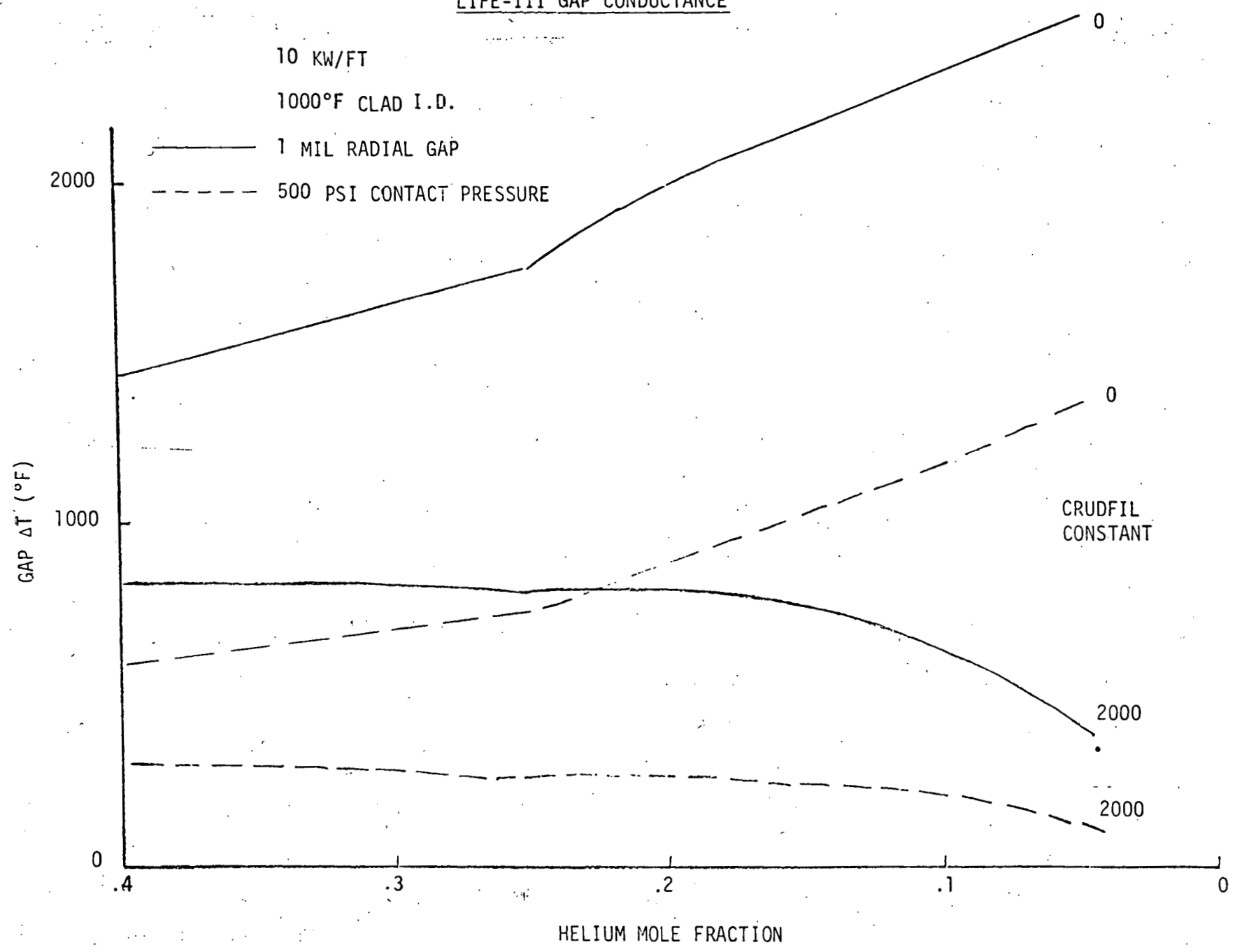
- a. gap conductance
- b. gas release and fuel swelling
- c. fuel creep
- d. cladding irradiation-induced deformation

TABLE 1-1 RESULTS OF LIFE-III CALIBRATION

	<u>OBSERVATIONS</u>			<u>LIFE-III</u>		
	<u>1*</u>	<u>2</u>	<u>3</u>	<u>1</u>	<u>2</u>	<u>3</u>
I - CLADDING DIAMETRAL INELASTIC STRAIN (%)						
WSA-2/13	.34	.48	.47	.40	.45	.66
WSA-2/17	.28	.51	.53	.31	.37	.38
P23A-25	.13	.18	.15	.05	.08	.12
F9A-5	-	.58	-	-	.23	-
F2V	.30	1.10	.90	.53	.81	.52
F9C-13	.03	.06	.06	.13	.18	.13
II - CENTER VOID RADII (MILS)						
WSA-2/13	0.	0.	0.	<1	<1	<1
WSA-2/17	0.	7	0.	<1	<1	<1
P23A-25	15	23	21	14	20	21
F9A-5	-	26	-	-	17	-
F2V	26	40	30	22	23	22
F9C-13	0	18	6	5	11	4
III - FISSION GAS RELEASE (%)						
WSA-2/13		50			61	
WSA-2/17		95			74	
P23A-25		95			86	
F9A-5		95			80	
F2V		~100			93	
F9C-13		79			73	

* axial location 1 = bottom of rod
 2 = core midplane
 3 = top of rod

FIGURE 1-1
LIFE-III GAP CONDUCTANCE



From the original LIFE-III creep model, power law creep is small relative to linear thermal creep at stresses below about 10,000 psi, and does not make a significant contribution to fuel deformation. An ongoing review of creep data indicates that the correlation for linear thermal creep predicts high creep rates. This is probably due in part to the interpretation of primary creep rates as steady state rates. The fission-enhanced creep correlation also seems to predict creep rates that are too high although the temperature dependency is satisfactory.

During calibration, the linear thermal creep component was reduced and its temperature dependency weakened in qualitative agreement with the results of the above review. The resulting model is shown as a tabulated creep map in Table 1-2. The LIFE-III temperature dependent grain size was used with the linear thermal creep component, and a uniform density of 90% was assumed. (The creep map shows the stress required to generate a given creep rate at a specified temperature).

The cladding irradiation-induced creep model was calibrated (an increase of 45%) and swelling predictions were adjusted to match immersion density measurements. As an alternate to this approach, the effects of temperature-dependent irradiation creep (J-creep) were investigated.

The results for cladding inelastic strains are similar, but with a tendency for J-creep analyses to show higher inelastic strains at high temperatures. The development of the J-creep model utilized a thermal creep model different from that contained in LIFE-III. There is therefore some uncertainty in the validity of the results obtained by combining the LIFE-III thermal creep and J-creep models. The results suggest that for a wide range of conditions the combination of the LIFE-III thermal creep and J-creep models yields acceptable results. However, it was decided to omit the J-creep model from the calibrated version of LIFE-III, although it will almost certainly be added later.

A brief study was made of the effects of varying the fuel and cladding analytical meshes on the primary variables studied during calibration. The following hypothetical test case was used:

TABLE 1-2

FUEL CREEP MAP WITH GRAIN SIZE = F(TEMP)
 ::::::::::::::::::::::::::::::::::::::

A1 = 3.833E+04 Q1 = 81935.0
 A2 = 1.000E-03 Q2 = 136800.0
 A3 = 2.800E-20 Q3 = 13700.0
 A4 = 3.720E-23

T / $\dot{\epsilon}$	1.000E-07	1.000E-06	1.000E-05	1.000E-04	1.000E-03	1.000E-02	1.000E-01	1.000E+00
1000.0	3.050E+01	3.050E+02	3.050E+03	3.050E+04	3.050E+05	3.019E+06	1.273E+07	2.384E+07
1100.0	2.215E+01	2.215E+02	2.215E+03	2.215E+04	2.214E+05	1.559E+06	3.343E+06	5.820E+06
1200.0	1.577E+01	1.577E+02	1.577E+03	1.577E+04	1.544E+05	5.677E+05	1.044E+06	1.785E+06
1300.0	1.122E+01	1.122E+02	1.122E+03	1.122E+04	9.222E+04	2.193E+05	3.858E+05	6.554E+05
1400.0	7.854E+00	7.854E+01	7.854E+02	7.842E+03	4.698E+04	9.473E+04	1.638E+05	2.776E+05
1500.0	5.249E+00	5.249E+01	5.249E+02	5.214E+03	2.390E+04	4.536E+04	7.787E+04	1.318E+05
1600.0	3.429E+00	3.429E+01	3.429E+02	3.369E+03	1.285E+04	2.373E+04	4.060E+04	6.868E+04
1700.0	2.276E+00	2.276E+01	2.276E+02	2.200E+03	7.358E+03	1.339E+04	2.285E+04	3.864E+04
1800.0	1.550E+00	1.550E+01	1.550E+02	1.468E+03	4.464E+03	8.040E+03	1.371E+04	2.317E+04
1900.0	1.082E+00	1.082E+01	1.082E+02	1.002E+03	2.847E+03	5.095E+03	8.677E+03	1.467E+04
2000.0	7.723E-01	7.723E+00	7.723E+01	6.998E+02	1.896E+03	3.378E+03	5.749E+03	9.715E+03
2100.0	5.627E-01	5.627E+00	5.627E+01	5.005E+02	1.311E+03	2.328E+03	3.961E+03	6.693E+03
2200.0	4.182E-01	4.182E+00	4.181E+01	3.662E+02	9.371E+02	1.660E+03	2.823E+03	4.770E+03
2300.0	3.167E-01	3.167E+00	3.166E+01	2.739E+02	6.892E+02	1.219E+03	2.072E+03	3.502E+03
2400.0	2.441E-01	2.441E+00	2.441E+01	2.091E+02	5.198E+02	9.182E+02	1.561E+03	2.637E+03
2500.0	1.913E-01	1.913E+00	1.913E+01	1.627E+02	4.008E+02	7.075E+02	1.203E+03	2.082E+03
2600.0	1.523E-01	1.523E+00	1.523E+01	1.298E+02	3.154E+02	5.563E+02	9.453E+02	1.597E+03
2700.0	1.230E-01	1.230E+00	1.230E+01	1.036E+02	2.525E+02	4.452E+02	7.565E+02	1.278E+03
2800.0	1.007E-01	1.007E+00	1.007E+01	8.454E+01	2.053E+02	3.619E+02	6.151E+02	1.039E+03
2900.0	8.343E-02	8.343E-01	8.341E+00	6.990E+01	1.694E+02	2.985E+02	5.072E+02	8.570E+02

$T = ^\circ K, \quad \dot{\epsilon} = h^{-1}, \quad \sigma = psi$

Linear power	15 kW/ft
Cladding O.D. temperature	1200°F
Fuel density	87%
Diametral gap	4 mils
Time (steady state)	10,000 hours (~12 a/o burnup)

The number of fuel regions was varied from 3 to 14 and the cladding regions from 5 to 9. (Calibration was performed using 12 fuel thermal rings, 6 fuel structural rings and 5 cladding rings.) The results (Table 1-3) show that the effect of varying the analytical mesh on observable parameters is smaller than the normally accepted precision of the experimental observations, i.e., about $\pm 0.05\%$ on diametral strains, ± 1 mil on center void size and $\pm 2\%$ on fission gas measurements.

The radial distributions of circumferential creep strain in the fuel were compared graphically for various fuel meshes. Inspection of the results (Figure 1-2) indicates that the strain profiles can be superimposed with very little scatter. Early in life, when a substantial amount of fuel cracking is still present, the strain profile with 3 fuel rings is slightly different from those using 6 or more rings, but the differences do not seem to have any practical significance.

From this brief ring sensitivity study it was concluded that:

- a) varying the analytical mesh from that used in calibration does not significantly influence the principal results generated; and
- b) for short history problems (<1 a/o), the effects of structural and thermal meshes may be more important than for longer running problems.

The effects of assumed uncertainties in the power and flux of two calibration rods (WSA-2/13 and F9A-5) were examined. Variations of $\pm 5\%$ in the nominal power and fluxes produced changes up to $\pm 8\%$ in the predicted cladding inelastic strains, but only very small changes in predicted center void sizes and quantities.

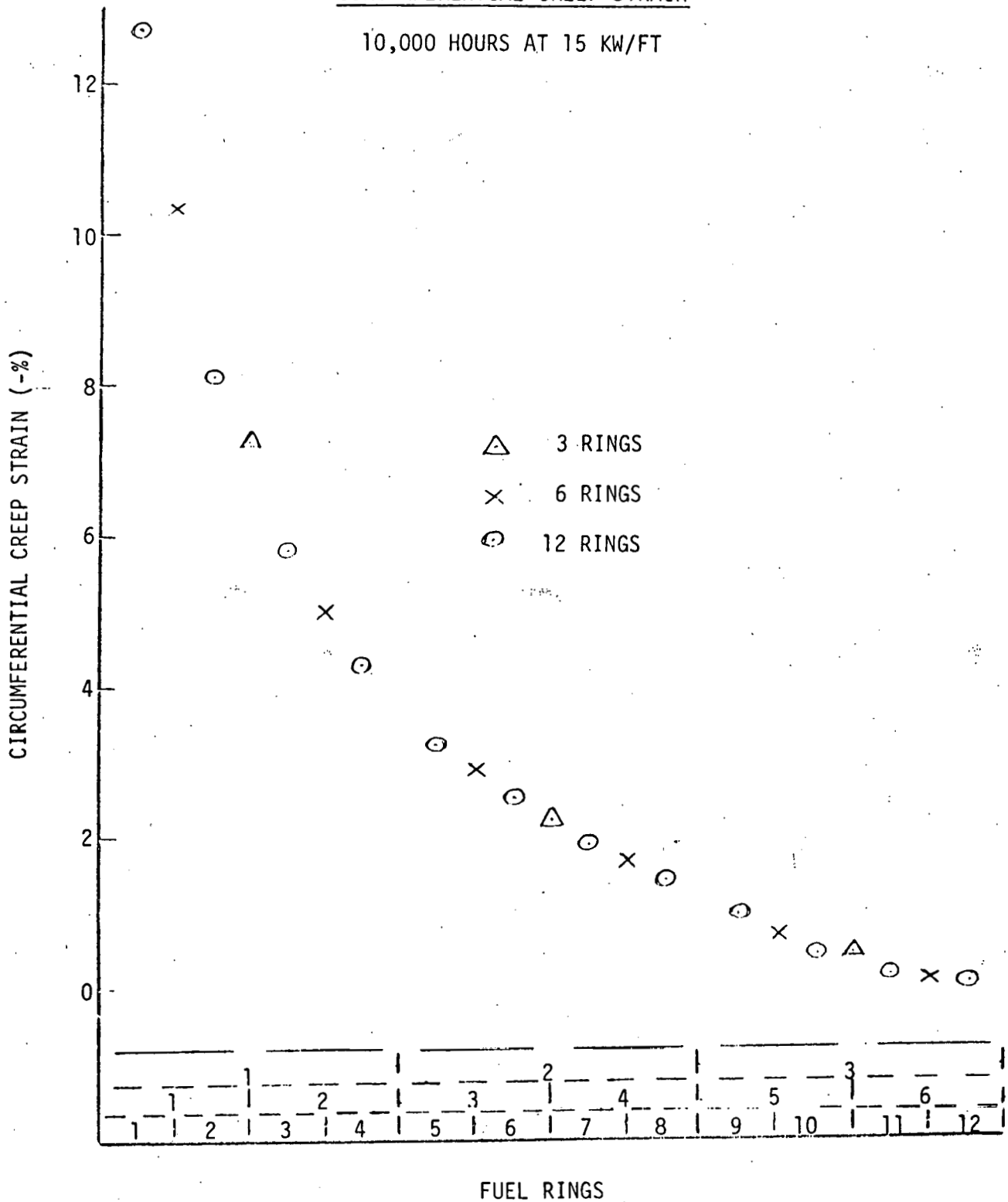
TABLE 1-3 RING NUMBER SENSITIVITY STUDY

GEOMETRY ^(a)	<u>3/3/5</u>	<u>6/6/5</u>	<u>6/12/5</u> ^(b)	<u>6/12/9</u>	<u>12/12/5</u>	<u>14/14/5</u>
Total $\Delta D/D(\%)$	3.952	3.951	3.984	3.989	3.981	3.983
Inelastic strain (%)	.229	.229	.262	.266	.262	.262
Center void (mils)	31.7	31.4	31.2	31.3	31.2	31.2
Gas release (moles $\times 10^2$)	.737	.737	.737	.737	.737	.737
EOL gap (mils)	3.25	3.28	3.31	3.32	3.31	3.31
Analysis Time (secs)	6	15	14	19	44	53

(a) X/Y/Z - X fuel structural rings
 Y fuel thermal rings
 Z cladding rings

(b) Standard geometry used in calibration.

FIGURE 1-2
RADIAL DISTRIBUTION OF
CIRCUMFERENTIAL CREEP STRAIN
 10,000 HOURS AT 15 KW/FT



A meeting was held June 4-5 at ERDA-RRD HQ to review LIFE development progress, and to do preliminary strategic planning for the development of a comprehensive system of fuel rod performance analysis codes. The major actions from the meeting which influence this subtask were:

- a. The LIFE-III calibration was accepted.
- b. The checkout of LIFE-III will proceed and be completed by November 1975.
- c. A preliminary development program for LIFE-IV will be defined by the LIFE Working Group.
- d. The LIFE Working Group will investigate the feasibility of using LIFE-III as the basis for a code to be used for the analysis of design transients.

Phase I of the checkout of LIFE-III using thirteen experimental rods is proceeding satisfactorily. Preliminary analytical results are shown in Table 4. The results for cladding inelastic strain show similar trends to those previously for the calibration rods.

Preliminary development requirements for LIFE-IV have been drawn up by the LIFE Working Group. The program will emphasize the development of new and improved fuel models to characterize behavior during the complete range of normal operation. It is anticipated that supplementary development needs will be identified from the results of the LIFE-III checkout. The preliminary development requirements are the following:

- a. Improvements to the fuel swelling model, including treatment of gas bubble growth and mobility and resulting deformations.
- b. A fuel creep model with the inclusion of the effects of all independent variables.
- c. A treatment of oxygen redistribution in the fuel, and the effects of oxygen content on fuel properties.

TABLE 1-4 LIFE-III CHECKOUT MECHANICAL ANALYSIS RODS

OBSERVATION	PEAK POWER (kw/ft)		CLAD. O.D. TEMPERATURE °F		VOID RADIUS (MILS)		MELT RADIUS (MILS)		COLUMNAR GRAIN RADIUS (MILS)		EQUIAXED GRAIN RAD. (MILS)		CLADDING DIA. INEL. STRAIN (%)		FISSION GAS RELEASE (%)	
	OBS	LIFE	OBS	LIFE	OBS	LIFE	OBS	LIFE	OBS	LIFE	OBS	LIFE	OBS	LIFE	OBS	LIFE
FUEL ROD																
WSA2-13	---	7.87	---	1061	0	.3	---	---	---	1.3	---	3.94	.48	.45	50	61.0
WSA2-17	---	9.759	---	1026	7	.3	---	---	---	1.3	---	7.22	.51	.37	95	74.18
WSA2-8	---	9.108	---	1074	-	.154	---	---	---	1.154	---	55.74	.32	.682	--	65.604
P23A-25	---	11.69	---	1312	23	20.40	---	---	---	75.65	---	83.95	.18	.08	95	86.25
GE F9A-5	---	16.78	932	968.7	26	18.44	---	---	---	84.31	---	89.82	.58	.23	95	79.56
NUMEC D-5	14.0	13.921	---	914	53	31.10	---	---	108	94.56	117	107.95	5.64	3.1	98	99.78

TABLE 1-4(CONT'D.) LIFE-III CHECKOUT THERMAL ANALYSIS RODS

OBSERVATION FUEL ROD	PEAK POWER (kw/ft)		CLAD. O.D. TEMP. (°F)		VOID RADIUS (mils)		MELT RADIUS (mils)		COLUMNAR GRAIN RADIUS (mils)		EQUIAXED GRAIN RADIUS (mils)	
	OBS.	LIFE	OBS.	LIFE	OBS.	LIFE	OBS.	LIFE	OBS.	LIFE	OBS.	LIFE
F20-S3	19.9	19.083	1147	-----	25.0	24.25	---	-----	85.5	87.14	102.5	89.14
P19-17R	18.3	17.20	1103	1109	30.5	23.82	32.5	----	82.5	87.34	96.5	89.34
P19-29	19.0	19.758	1161	1146	11.5	9.72	42	18.34	74.0	65.65	86.0	67.65
F20-C2	19.6	19.015	1124	1139	30	27.56	---	-----	85.0	87.83	105.5	89.83
F20-E5	20.3	19.370	1147	1154	9	20.72	43	----	82.5	84.71	101.0	86.71
F20-E8	---	15.78	---	1126	--	21.85	---	-----	---	85.55	----	85.56
F20-C11	---	16.59	---	1151	--	21.81	---	-----	---	86.90	----	88.90
P20-33	---	18.834	---	1152	20.0	18.50	21.3	----	78.0	75.14	----	75.32
P19-28	21.37	20.829	---	1031	26.7	15.04	36.0	28.66	73.3	78.65	----	80.65
04-431-DP1	11.16	10.89	649	979	---	1.67	---	-----	---	2.67	----	23.68

- d. Revision of the gap conductance model, including an improved description of solid fission product deposits.
- e. Improvements to the fuel cracking model such as stress affected crack healing and anisotropic effects.
- f.* Solid fission product swelling and the effects of solid fission products.
- g.* Cladding damage calculations.
- h. The influence of swelling "porosity" on fuel properties and behavior.
- i.* Analytical limitations of property models and correlations, and possible extrapolation methods.
- j. Further improvements (as necessary) to the treatment of the fuel-cladding boundary condition analysis.
- k. Improvements to the efficiency of the code algebra.

1.1.2 Transient Analysis

LIFE-III is being considered for use as the basis for development of a national code to analyze fuel rod behavior during design basis transients up to cladding breach. The two primary advantages of this approach are:

1. Utilization of the large body of experience accumulated during the development of LIFE-III could give the transient code development a substantial headstart, over a starting-from-scratch approach.

*These activities will involve strong interactions with the NSMH committees.

2. Transient analyses with a LIFE code would be automatically interfaced with steady state behavior analyses during the pre- and post-transient periods.

It is clear that LIFE-III lacks both models and analytical techniques that are necessary to perform meaningful analyses of fuel rod behavior during transient operating conditions. GE has studied these deficiencies and has attempted to evaluate the feasibility of correcting them while taking the fullest advantage of the first advantage of LIFE noted above. The evaluation is jointly based on engineering judgments developed from experience gained in the construction and utilization of the LIFE and BEHAVE codes. The latter was developed by, and is in current use at GE for the analysis of fuel rod transient behavior under the Safety Engineering Program.

Design basis transients - overpower and loss of flow - have been defined, and some estimates are presented to show the impact of the TOP events on fuel and cladding temperatures. These results are used to define the limiting physical conditions that the LIFE transient code would be required to model. The principal limiting conditions are:

1. Relatively small amounts of fuel melting (not more than 50% of the cross-section area).
2. No cladding melting.
3. No sodium boiling.
4. Behavior up to the point of cladding breach.

The principal development requirements for a LIFE-based transient analysis code are as follows.

A new thermal analysis system is required to treat time-dependent heat transport, and to provide thermal axial coupling through the coolant. The BEHAVE-3 thermal analysis system could be readily adapted for use in LIFE.

Models and analytical methods are required to treat high strain rate deformation. Either primary creep or time-independent plastic flow approaches could be used, with the former preferred.

A new model must be identified for transient fuel swelling and gas release. The complexity of this model should be minimized.

The importance of fuel cracking in determining transient fuel rod behavior requires improvements be made to the LIFE-III model to take account of the anisotropic properties of cracked fuel, and the differences in stress states between solid and cracked fuel.

Coupling of the thermal and mechanical analyses may be a critical feature of the transient code, and a satisfactory way of achieving this must be devised.

A simplistic treatment of molten fuel behavior is favored, especially as relatively little melting is anticipated.

If any of these development requirements would cause the bulk of LIFE-III to be reconstructed, the primary advantages would be lost. However, after reviewing these requirements, it has been concluded that no problems can be identified which would preclude the use of LIFE-III as the basis for the development of a code to predict fuel rod behavior during design basis transients.

It is necessary to determine the scope of fuel behavior that must be modeled by the transient code. If the cladding and sodium temperatures are below the melting and boiling points, respectively, and no gross fuel movement occurs, the requirements for the transient code are simplified. The credible design transients which have to be analyzed are as follows:

1. 30¢ step positive reactivity insertion
2. 10¢/sec up to \$2 total positive reactivity insertion
3. The step flow reduction associated with the instantaneous loss of coolant from one primary loop. (1-2)
4. Loss of electrical power with pump coastdown. (1-2)

The design transient code to be developed should, as a minimum, be able to analyze these credible transients. In addition, it is noted that CRBRP is considering as a design basis, overpower events which are associated with no identifiable physical processes. These hypothetical overpower events include 60¢ step reactivity insertion and a \$2/sec transient. In the FFTF design, the even more hypothetical \$3/sec transient overpower event has been used as a design basis for the fuel rod emergency overpower design. Although as stated, the above overpower events being considered in the design of the CRBR and FFTF fuel rods are hypothetical, it is considered desirable that the design transient code to be developed should, if possible, be able to properly analyze these severe hypothetical overpower transients.

To identify transient fuel rod conditions, the above TOP and TUC events were analyzed for a typical LMFBR design. Coupled neutron kinetics - thermal hydraulics calculations have been performed with the FOXE-II code (similar to FORE-II [1-3]), and the BEHAVE-3 (1-4, 1-5) code has been used for fuel rod transient thermal and structural analyses. Pretransient conditions for a typical fuel rod operating at 12.5 kw/ft were utilized. The sodium inlet temperature and temperature rise across the core were 385°C and 180°C, respectively. A reference scram delay time of 0.15 second was selected (1-6). A reference scram insertion time of 1.6 seconds was based on the CRBR design (1-7). The secondary scram system inserts control rods in 1.2 seconds (1-7).

Calculational results were obtained using the fuel rod pretransient conditions and the reference scram insertion and delay times. Figure 1-3 illustrates the reactor power and the fuel and cladding core midplane temperatures as a function of time for a \$3/second transient overpower event in which a total reactivity of \$2 was inserted. Peak temperatures and heating rates for \$1/second, \$2/second, and \$3/second transients are summarized in Table V. Calculations indicate that temperatures in the TUC events are similar to or less than those produced in the \$1/second TOP.

It is concluded from these results that the \$3/second terminated transient overpower event produces the most severe conditions in the fuel rod. The peak cladding temperature at the top of the fuel rod, 791°C is well below the melting point of the cladding, approximately 1300°C. No sodium boiling is indicated. BEHAVE contains a fuel motion model and no fuel movement was predicted. Modeling of these phenomena are, therefore, not required in the transient code. In addition, no fuel melting was predicted, but in view of the closeness of the calculated peak fuel temperature to the melting range of mixed-oxide fuel, approximately 2760°C to 2840°C, it is felt that a capability for handling molten fuel must be incorporated into the transient code.

It should be noted, however, that some fuel melting will occur during a transient if higher pretransient fuel centerline temperatures exist, or scram delay times are longer. For instance, initial fuel centerline temperatures of 2400°C will cause 7% of the fuel to melt during a \$3/second transient. Increasing the scram delay time by 200 msec during a \$3/second transient may cause melting in 10% to 15% of the fuel volume, and produce approximately 20% areal fuel melting at the core midplane. BEHAVE tended to predict motion of small amounts of fuel from the core midplane to the ends of the rod when the molten fuel volume exceeded 10%.

Results of previously conducted transient overpower experiments should also be examined to assess the limits of fuel behavior that can be expected for design basis transients. The GE C-Series (1-8 through 1-12) experiments performed at TREAT are currently being reviewed.

FIGURE 1-3
CONDITIONS DURING \$3/S COND DESIGN TRANSIENT

\$3/SEC TRANSIENT OVERPOWER

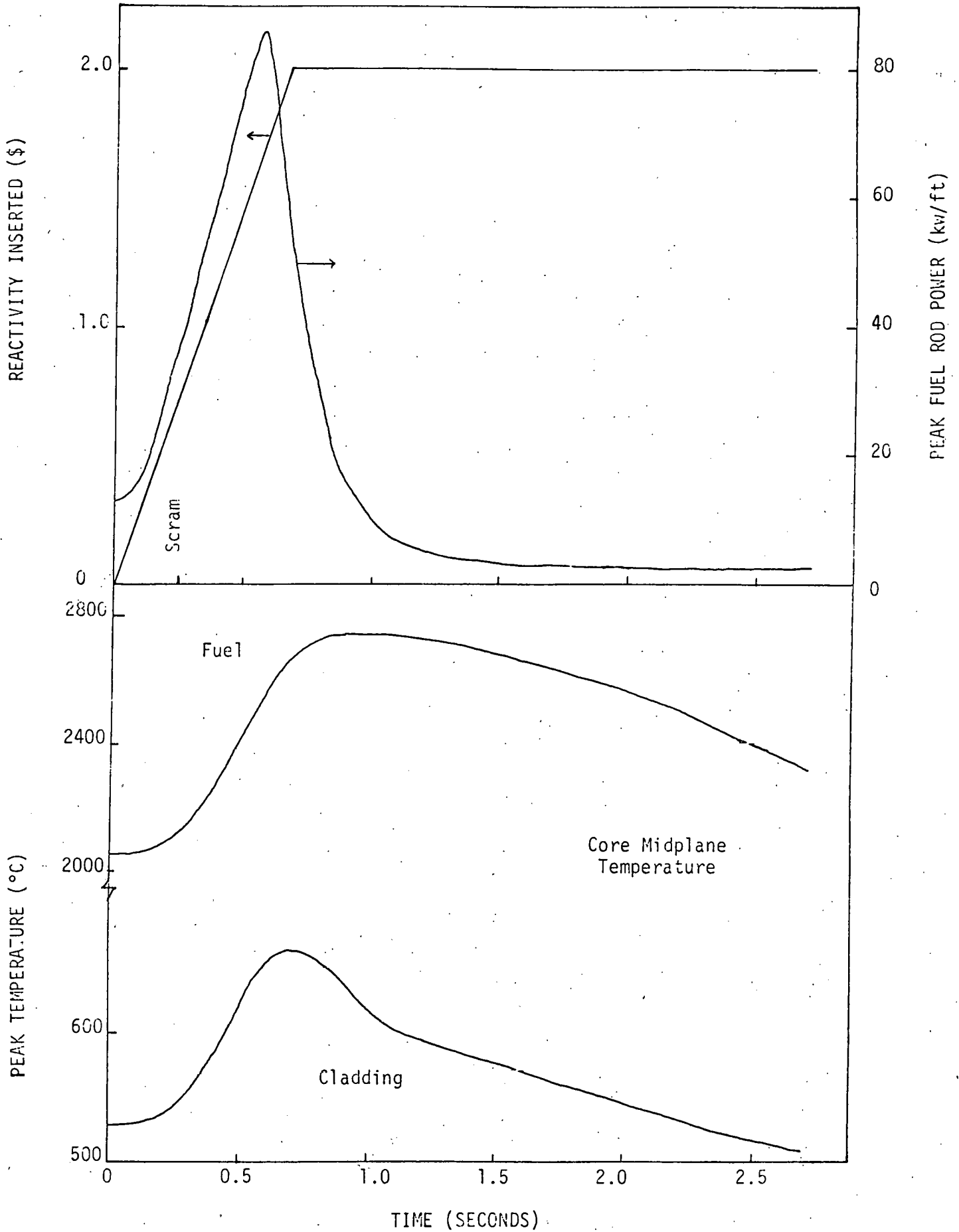


TABLE 1-5

SUMMARY OF DESIGN BASIS TRANSIENT
CALCULATIONS FOR A TYPICAL LMFBR

PARAMETER (VALUE AT CORE MIDPLANE UNLESS OTHERWISE SPECIFIED)	REACTIVITY INSERTION RATE (\$/SEC)		
	1	2	3
Peak power (kw/ft)	22.1	38.9	85.5
Peak power increase rate (kw/ft/sec)	42	65	164
Peak fuel temperature (°C)	2222	2408	2739
Peak fuel heating rate (°C/sec)	266	680	1580
Peak cladding temperature (°C)	555	585	663
Peak cladding heating rate (°C/sec)	50	160	437
Peak cladding temperature (°C) (top of fuel rod)	638	682	791
Peak temperature difference across cladding (°C)	34	38	54
Peak sodium temperature (°C)	505	526	584
<u>Pretransient Conditions at Core Midplane</u>			
Peak power (kw/ft)	12.5		
Peak fuel temperature (°C)	2050		
Peak cladding temperature (°C)	528		
Peak sodium temperature (°C)	485		

1.2 FUEL ROD DATA EVALUATION

1.2.1 Fuel Rod Failures

The objective of this activity is to develop failure criteria for LMFBR fuel rods. The fuel-cladding mechanical interaction code GRO-II was modified to include thermal expansion of the inviscid zone as a loading mechanism.

1.2.2 Fuel Rod Cladding Inelastic Strain

The objective of this activity is to determine the relative contribution of various loading mechanisms to the observed cladding inelastic strain in fuel rods.

Preliminary analyses to evaluate the observed cladding inelastic strains in fuel rods from GE, ANL and UK experiments have been completed. Cladding inelastic strain predictions based on fission gas pressure only consistently underestimate the measured inelastic strain. Prediction of cladding inelastic strains based on the mechanism of fuel-cladding mechanical interaction is in progress.

A memo report, "Cladding Inelastic Strain in Mixed Oxide Fuel Rods: Literature Review and Data Compilation", was completed and forwarded to RRD.

1.2.3 Fuel Rod Thermal Performance

The near-term objective is to conduct the National Experiment Evaluation Program of the F20 power-to-melt experiment.

The performance of several representative rods from the F20 experiment has been analyzed using LIFE-III. The analyses tend to underpredict fuel temperatures as evidenced by the occurrence and extent of melting. This may be partially due to the difficulty in accurately reproducing the experimental operating conditions. Methods to increase the flexibility of the LIFE description of operating conditions were developed. These allow the axial power shape to be modified during the run history, and new cladding O.D. temperatures to be input as required.

The results shown in Table 1-6 using the new input techniques still show underpredictions of fuel temperatures for the Phase I and II rods, but reasonably good predictions for the Phase II only rods. The results for F20-S3 (I and II) and F20-P19/29 (II) are shown in Figure 1-4. Both rods showed fuel melting during the Phase II exposure, but LIFE-III predicts no melting in F20-S3. The analysis of this rod predicts fuel-cladding gap closure during Phase I due to the high rate of early-life fuel swelling. Experimental measurements show that the initial diametral fuel-cladding gap decreased from 6 to about 4 mils, indicating that the fuel and cladding were probably not in contact at the end of Phase I. The requirement for the fuel swelling model to close the initial gap more slowly, and still load the cladding sufficiently to generate inelastic strains are in conflict with the formulation of the current model. Modifications to the model to simulate an incubation period before swelling starts are being developed.

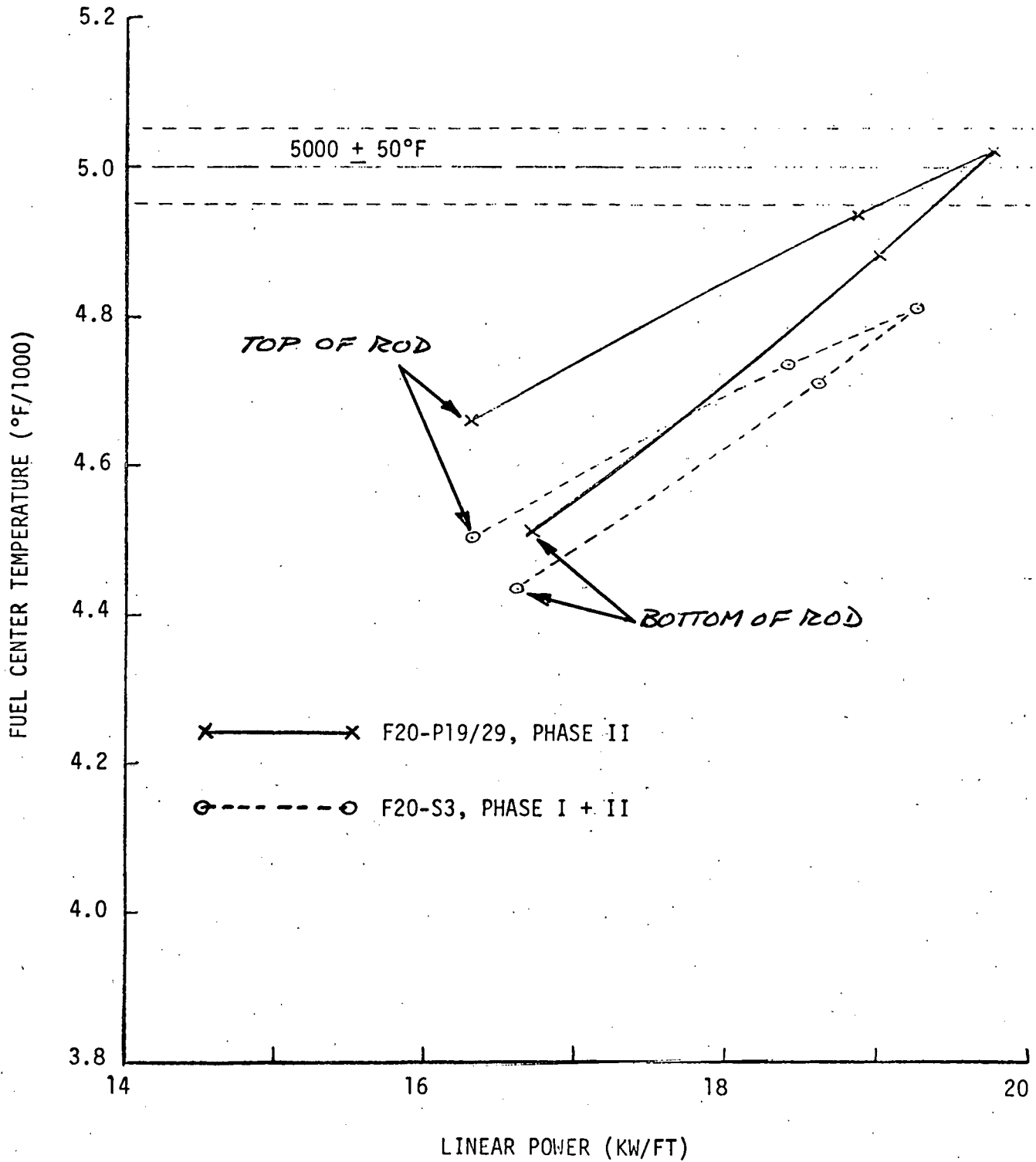
TABLE 1-6 F20 POWER-TO-MELT EXPERIMENT LIFE-III ANALYSIS

OBSERVATION FUEL ROD	PEAK POWER (kw/ft)		CLAD. O.D. TEMP. (°F)		VOID RADIUS (mils)		MELT RADIUS (mils)		COLUMNAR GRAIN RADIUS (mils)		EQUIAXED GRAIN RADIUS (mils)	
	OBS.	LIFE	OBS.	LIFE	OBS.	LIFE	OBS.	LIFE	OBS.	LIFE	OBS.	LIFE
F20-S3	19.9	19.083	1147	----	25.0	24.25	----	----	85.5	87.14	102.5	89.14
P19-17R	18.3	17.20	1103	1109	30.5	23.82	32.5	----	82.5	87.34	96.5	89.34
P19-29	19.0	19.758	1161	1146	11.5	9.72	42.0	18.34	74.0	65.65	86.0	67.65
F20-C2	19.6	19.015	1124	1139	30.0	27.56	----	----	85.0	87.83	105.5	89.83
F20-E5	20.3	19.370	1147	1154	9.0	20.72	43.0	----	82.5	84.71	101.0	86.71
F20-E8	*	15.78	----	1126	----	21.85	----	----	----	85.55	----	85.56
F20-C11	*	16.59	----	1151	----	21.81	----	----	----	86.90	----	88.90

*Note: There is currently no post-irradiation examination data available for F20 rod E8 and C11.

FIGURE 1-4

LIFE-III ANALYSIS OF GE F20 RODS



1.3 FUEL AND STRUCTURAL MATERIAL PROPERTIES DESIGN CORRELATIONS

1.3.1 Thermal Conductivity of (U,Pu)O_{2-x} Fuels

A previous report (1-13) has highlighted the effects of porosity gas on the measured mixed-oxide thermal conductivity. That study showed that the presence of helium in the porosity of mixed-oxide fuel results in significantly enhanced thermal conductivity over that for argon-filled porosity. The presence of He in these measurements being biased somewhat higher in value than those of other experimenters who used argon during specimen fabrication and experimentation.

Marino (1-14) has treated the porosity gas problem in terms of the pore shape factor, β , which depends upon the ratio of the porosity gas conductivity and the oxide conductivity as well as the ratio of the semi-minor and semi-major axes of pore ellipsoids distributed randomly throughout the oxide. As shown in reference 15 differences in the gas in porosity of the oxide specimens could explain the lack of variability due to density changes in the GE thermal conductivity data.

The available thermal conductivity data are not sufficiently complete to allow a precise analysis of specimen porosity. Thus, some empiricism is necessary in handling the data to place it on a consistent basis. An examination of the GE data (1-15) indicates that a reasonable value for the porosity eccentricity factor is about

$$\epsilon = \frac{\text{Semi-minor axis}}{\text{Semi-major axis}} = 0.15 \quad (1)$$

In lieu of prior knowledge of microstructural information on the vast majority of the available thermal conductivity data, the above value of ϵ was assumed to be reasonable for all specimens.

Once this assumption was made, a plan could be carried out to eliminate density as a variable in thermal conductivity by the following procedure:

1. Using a value $\epsilon = 0.15$, a value for β was found for each data point assuming helium as a pore gas for GE data and argon as a pore gas for all other data.

2. Each data point was then adjusted to 100% of theoretical density using the relationship (1-14)

$$K_{100} = (K_{\text{measured}}) \frac{(1+\beta\rho)}{(1-\rho)} \quad (2)$$

where ρ = porosity

3. The 507 data points were then fit to a regression equation of the form shown below using the BASIC program MULFIT.

$$K_{100} = \frac{1}{A+BT+CX} + DT^3 \quad (3)$$

where T is temperature in degrees centigrade and $X = (2.0 - O/M)$

Since MULFIT can handle only linear equations directly, equation (3) was linearized by subtracting the T^3 term from the righthand side of the equation and then taking the reciprocal. The value of D was found by iteration. The regression analysis resulted in the following equation for K_{100}

$$K_{100} = \frac{1}{8.3233 + .027078T + 195.67X} + 1.1572 \times 10^{-12} T^3 \quad (4)$$

The form of equation (3) is partly based on the assumption of phonon scattering by thermal defects and lattice defects introduced through nonstoichiometry as discussed at length by Gibby (1-16). The T^3 term as discussed by Schmidt (1-17) may be due to an increase in the specific heat of the mixed oxide caused by the electronic component. Ainscough (1-18), however, is examining those measurements carried out using a radial heat flow technique (such as used by GE), points out that in those tests where the fuel specimens are heated electrically by means of a center electrode, electrical conduction in the oxide itself at high temperatures could lead to erroneously high measured conductivity values. Thus, the upswing in thermal conductivity observed at high temperatures (T^3 term) may be illusory.

The form of equation (4) is convenient in that fuel rod analyses may be carried out to study the effects of fission gas on the overall thermal conductivity of the porous oxide simply by adjusting the parameter β to the proper value.

The final equation, including the porosity effect, has the form

$$K = \frac{1-P}{1+\beta P} \left[\frac{1}{8.32377 + 0.0270783T + 195.6729 (2-O/M)} + 1.15715 \times 10^{-12} T^3 \right] \quad (5)$$

K = thermal conductivity (watts/cm°C)

T = temperature (°C), (800-2400°C)

P = porosity (0 to 0.16) (1.-fractional density)

O/M = stoichiometry (1.93 to 2.00)

β = porosity shape factor

Pu mole fraction 0.2 to 0.3

Standard deviation of residuals from regression equation = 2.367×10^{-3}

95/95 tolerance interval $\pm 4.92 \times 10^{-3}$

A submittal to the Nuclear Systems Materials Handbook, "Thermal Conductivity of $UO_2 - PuO_2$ " was drafted and internal review initiated.

1.3.2 Oxygen Redistribution and Thermal Performance

The above equation for thermal conductivity has been used to measure the effect of oxygen redistribution on the fuel thermal performance. An existing program for calculating oxygen redistribution was modified to take into account changes in thermal conductivity equation (equivalent to the average stoichiometry resulting from oxygen redistribution.)

The aim of the calculations was to determine the effects of such manipulations on the calculated power-to-melt. The calculation using the correct thermal conductivity (making adjustments in the equation as oxygen redistributes) results in a power-to-melt up to ~ 0.85 kW/ft higher than if a constant stoichiometry is used in the thermal conductivity expression.

REFERENCES

- 1-1. D.S. Dutt, R.B. Baker and S.A. Chastain, "Modeling of the Post-Irradiation Fuel-Cladding Gap in Mixed Oxide Fuels," HEDL-TME-74-19, April 1974.
- 1-2. CRBR PSAR, Chapter 15.
- 1-3. J.N. Fox, B.E. Lawler and H.R. Butz, "FORE-II, A Computational Program for the Analysis of Steady-State and Transient Reactor Performance," GEAP-5273, 1966.
- 1-4. S. Oldberg, Jr., "BEHAVE-2: Oxide Fuel Performance Code in Two Spatial Dimensions and Time," GEAP-13788, 1972.
- 1-5. R.G. Stuart and S. Oldberg, Jr., "Steady State and Transient Fuel Mechanics; The BEHAVE-3 Code," GEAP-14021, 1974.
- 1-6. FFTF PSAR, Chapter 15.
- 1-7. CRBR PSAR, Chapter 4.
- 1-8. J.E. Hanson, J.H. Field, S.A. Rabin, "Experimental Studies of Transient Effects in Fast Reactor Fuels, Series II, Mixed Oxide ($\text{PuO}_2\text{-UO}_2$) Irradiations," GEAP-4804, 1965.
- 1-9. J.E. Hanson and J.H. Field, "Experimental Studies of Transient Effects in Fast Reactor Fuels, Series III, Pre-Irradiated Mixed Oxide Irradiations," GEAP-4469, 1967.
- 1-10. G.R. Thomas and J.H. Field, "Transient Overpower Irradiation of Axially Restrained Zero-Burnup Fast Reactor Fuel Specimens," GEAP-13562, 1970.
- 1-11. T. Hikido and J.H. Field, "Molten Fuel Movement in Transient Overpower Tests of Irradiated Oxide Fuel," GEAP-13543, 1969.
- 1-12. T. Hikido and J.H. Field, "Performance Tests of Sodium Filled, Powder, and Pellet Oxide Fuel Under Transient Overpower," GEAP-13722, 1971.
- 1-13. Reference Fuel Studies (Task 3) quarterly report for period ending January 31, 1975.
- 1-14. Marino, G.P., "The Porosity Correction Factor for the Thermal Conductivity of Ceramic Fuels," J. Nucl. Matl., 38, 178-190 (1971).
- 1-15. Laskiewicz, R.A., Melde, G.F. Evans, S.K., and Bohaboy, P.E., "Thermal Conductivity of Uranium-Plutonium Oxide," General Electric Company, September 1971 (GEAP-13733).

The gap conductance model was modified to simulate the improvement in heat transfer which may be expected from the deposition of solid fission products at the fuel-cladding interface. The primary effect of this model change is to suppress a tendency to predict unrealistically high fuel temperatures if the cladding swells away from the fuel at high burnups. Fuel microstructures in GE-F2V showed no evidence of melting or very high surface temperatures. A so-called CRUDFIL constant was adjusted during calibration to improve gap conductance to the required degree. Without the CRUDFIL change, the gap ΔT increases continuously with increasing fission gas content, but with CRUDFIL = 2000 (the calibrated value) this trend is reversed when the fission gas fraction exceeds 0.7 (Figure 1-1). The calibration rod data do not permit definitive judgment of the validity of this effect. However, it will be possible to evaluate the high burnup gap conductance model using data on the thermal performance of moderate to high burnup fuel rods tested in the GE-F20 experiment.

The calibrated fuel swelling model predicts saturation volume increases under constant ambient conditions. The saturation volumes decrease with increasing temperature. These qualitative features of the model are in agreement with those expected from fundamental fission gas behavior in fuel in the presence of a temperature gradient. The swelling rates predicted by the LIFE-III model result in very rapid gap closure. Measurements of residual gaps (1-1) suggest that gap closure is much slower than is predicted by LIFE-III. Although the rate of gap closure alone in the calibration rods has little effect on the predicted cladding inelastic strains, it has a noticeable effect on the early life thermal performance. Further studies of fuel swelling behavior and its effects are being conducted as part of the LIFE-III checkout program.

The LIFE-III description of fuel creep behavior uses the sum of four steady state mechanisms:

- a) linear thermal creep ($\dot{\epsilon} \propto \sigma$),
- b) power law thermal creep ($\dot{\epsilon} \propto \sigma^{4.4}$),
- c) temperature dependent fission-enhanced creep,
- d) a thermal fission-induced creep.

- 1-16. Gibby, R.L., "The Effect of Oxygen Stoichiometry on the Thermal Diffusivity and Conductivity of $U_{0.75}Pu_{0.25}O_{2-x}$," Battelle Memorial Institute, January 1969 (BNWL-927).
- 1-17. Schmidt, H.E., "Some Considerations on the Thermal Conductivity of Stoichiometric Uranium Dioxide at High Temperatures," J. Nucl. Matl., 30, 234-237 (1971).
- 1-18. Ainscough, J.B., "The Effect of Electrical Conduction in UO_2 on the Measurement of Its High Temperature Thermal Conductivity as Determined by Radial Flow Techniques," J. Nucl. Matl., 20, 184-192 (1966).

MAJOR CONTRIBUTORS

D. W. Croucher
S. K. Evans
R. F. Hilbert
O. M. Hopkins
W. S. Lovejoy
M. R. Patel
S. O. Peck
R. G. Sim
J. D. Stephen
J. E. Turner
N. M. Tuttle

189 NO. SG009 - FUELS IRRADIATION TESTING AND ANALYSIS

Cognizant Engineer: W.H. McCarthy

SUMMARY

F8B Subassembly X117B was successfully dismantled in HFEF-North. No breached claddings were detected.

A data package for the continued irradiation of 34 unencapsulated high-cladding temperature series F11A rods was mailed to the EBR-II Project. There is a good probability that this reirradiation can start in Run 79.

The maximum rod in Experiment F9C-1 (X143) achieved 17.8% estimated burnup in Run 77.

Memorandum reports were issued on the fuel redistribution and microstructure in F20 rods and on the present status of the encapsulated rods that exhibited cladding breach.

Two topical reports have been drafted. The report on the F9 results is in publication. Internal review of the F6/F8 low linear power experiment report is in process.

2. FUELS IRRADIATION TESTING AND ANALYSIS

Cognizant Engineer: W.H. McCarthy

The objective of fuels irradiation testing and analysis is to determine experimentally fuel rod behavior under fast-flux irradiation. The work is focused on supporting the core design for FTR and CRBR Plants. The irradiation tests provide data for development of design correlations in five general areas: High Burnup Irradiations, Low Power Irradiations, High Cladding Temperature Irradiations, and Operating Limits Irradiations. Cognizance of the overall US-ERDA LMFBR program and foreign programs is emphasized so that the work provides information which complements that obtained from other programs.

2.1 HIGH BURNUP IRRADIATIONS

The F9C-1 (X143A) and F9D-1 (X204) experiments were irradiated in EBR-II run 77, and they are continuing in Run 78. Run 77 was an extra-long cycle (~ 3600 instead of 2700 MWd). To date, no GE experiment has caused any EBR-II outage of a fission gas leak. The estimated maximum rod axial peak burnup values for F9C-1 and F9D-1 were 17.8% and 12.0%, respectively at the end of Run 77.

The data package for the F9A-1 experiment (X214) is being revised to call for 37 instead of 19 rods from X043A and X144. It will be proposed to use reactor location 6D1 which, since it is adjacent to the dummy control rod (and not adjacent to an active control rod), will allow a plenum pressure limitation of 1000 psi. (The limit adjacent to an active control S/A is 450 psi.) The 37-rod configuration will help to solve both the reactivity problem in the reactor and the rod storage problem when HFEF-South is shut down for a major overhaul.

A data package for the reirradiation of thirty-seven F9B and F9D rods from X062A and X048 also is being prepared. This subassembly will operate at lower power than F9A-1. Nondestructive examinations have been performed on some of the F9A, F9C and F9D rods recently shipped to LASL.

PNL has concluded from its COBRA-IV analysis that flow coastdown Test F resulted in an isothermal sea condition that was not deleterious to the experiments. GE has expressed its concurrence with this finding to the EBR-II Project.

A topical report describing the irradiation of the F9A, -B, -C and -D series of unencapsulated fuel rods (through Run 75), and the destructive examination of nine of these rods, was completed. These rods have been irradiated in the following irradiation vehicles: X043(A) (~ 9% burnup), X056(A) (~ 6%), X058 (8%), X062(A) (11%), X143(A) (17%), and X204 (12%). Destructive examination results on selected rods from the first four subassemblies listed above are included in the report. X143A and X204 are the run-to-cladding breach experiments still being irradiated, and most rods from X144 will be incorporated in the F9A-1 experiment (X214). Selected X144 rods will be destructively examined without further irradiation after the reirradiation plans for the remaining X144 rods have been approved. The major conclusions of the report are:

- (a) These rods are still in good condition after being subjected to irradiations up to 10 at.% burnup.
- (b) Inelastic cladding strains (total strain less the metal swelling component) of 0.8% were measured without cladding rupture.
- (c) Maximum depth of fuel/cladding chemical interaction was 0.0004 inch.
- (d) Normal fuel microstructural features were found after the irradiation of both coprecipitated and mechanically blended mixed-oxide fuels.
- (e) Subassembly duct-to-rod-bundle clearance (or interface) can be predicted from the dimensions of the components and the irradiation history. Results indicate that initial bundle-to-duct clearances of 0.014 inch are tight enough to prevent appreciable fretting wear of the rods by the wrapping wires.

LOW POWER IRRADIATIONS

Subassembly X117B containing six encapsulated F8B series rods was disassembled at HFEF-North. This is the first GE irradiation vehicle to be handled at this new facility. The disassembly proceeded very smoothly, and the capsules appeared to be in good condition, although they were quite bowed. Visual examination, gross gamma scanning, and neutron radiographic examinations are now going forward.

The rods were cooled too long to get meaningful leak-checking gamma scanning from Xe in the capsule plena. Scanning of the capsule sodium above the top insulator for Cs¹³⁷ indicated, however, that there was no cladding breach in any X117B rod.

Seven series F8B encapsulated low power rods were irradiated in Run 77 (X118A). They are expected to reach their goal burnup of 11.2% during Run 78. Companion rods are at LASL for destructive examination. This experiment will provide data on the continued operation of low power rods after a midlife overpower exposure of as much as 33%.

A topical report on the F6 and F8 irradiations (X010 and X019) and post-irradiation examinations was prepared and is going through internal management review. The experiment demonstrated that low power (< 10 kW/ft) rods can be irradiated to moderate burnup (5 at.%) without difficulty. Small amounts of fuel/cladding mechanical interaction were reported.

F9B was discussed under HIGH BURNUP IRRADIATIONS.

BREACHED CLADDING

The post-irradiation examination of 15 encapsulated rods with breached cladding is continuing at LASL. No new failures have been found. No unencapsulated GE rod has yet exhibited a cladding breach. A memorandum report defining the current status of the breached rods has been issued. The principal conclusion of this report is that the change in power profile, when the radial reflector was inserted at Run 56, was the principal contributing factor to the cladding breaches in these 15 encapsulated rods. The data from one rod (F8L) indicate that localized overheating may also have been important.

HIGH CLADDING TEMPERATURE IRRADIATION TESTS

F10A-1 Experiment

Material has been procured for the triangular flow restrictors to be inserted in the edge channels of F10A-1 irradiation vehicle (X121A). These restrictors will provide the required radial uniformity of coolant temperature that was

maintained in the previous F10A and F10B irradiations (X121 and X122). It is expected that sufficient parts will be shipped to EBR-II, Chicago, early in August 1975, for fabrication of the flow test mockup and the subassembly. The plans call for the irradiation to resume in Run 80.

F11A Experiment

The destructive examination of three F11A (X141) unencapsulated high cladding temperature rods is proceeding at LASL. Preliminary nondestructive examination data (pulsed eddy current) indicated that there was no extensive intergranular attack at the inside surface of the cladding. Two rods have been cross sectioned. The data package for continued irradiation of the remaining thirty-four F11A rods (with three F9E series spares) was submitted to the EBR-II Project. The reirradiation is expected to begin in Run 79 (September 1975), provided the F9E spare rods are received from HEDL in sufficient time.

OPERATING LIMITS IRRADIATIONS

The destructive examination of (22) F20 rods is continuing at LASL. Detailed evaluation of the fuel microstructures is proceeding at GE. A paper on the self-healing of the axial redistribution of molten fuel by continued irradiation (Phase III) was presented at the ANS annual meeting June 12, 1975. A preliminary report covering this topic and initial F20 microstructural examination results for LIFE-III verification was issued.

MAJOR CONTRIBUTORS

N.H. Blumstein
S.E. Costanza
S.K. Evans
B.L. Harbourne
R.F. Hilbert
G.E. Hittle
D.K. Kerwin
C.B. Kincaid
D.E. Plumlee
N.M. Tuttle
D.C. Wadekamper